

Improving Selectivity in 2-Butyne-1,4-diol Hydrogenation using Biogenic Pt Catalysts

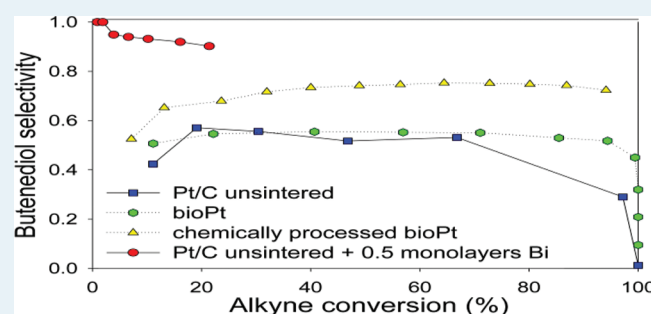
J. A. Bennett,[†] G. A. Attard,[§] K. Deplanche,[‡] M. Casadesus,[§] S. E. Huxter,[§] L. E. Macaskie,[‡] and J. Wood*[†]

[†]School of Chemical Engineering and [‡]School of Biosciences, University of Birmingham, Edgbaston, Birmingham B15 2TT, U.K.

[§]Cardiff Catalysis Institute, Cardiff University, Park Place, Cardiff CF10 3AT, U.K.

ABSTRACT: The selectivity towards 1,4-butanediol hydrogenation of both a standard 5 wt % Pt on graphite supported catalyst and a biogenic Pt analogue is reported. In both cases, it is determined using cyclic voltammetry that step sites afford the greatest extent of hydrogenation and that deliberate blocking of such sites gives rise to significant selectivity in favor of the 1,4-butanediol product. For the 5 wt % Pt/graphite catalyst, irreversible adsorption of bismuth was used as the step site blocking agent. In the case of the biogenic Pt nanoparticles (NPs) synthesized within the bacterium *Escherichia coli*, residual molecular organic fragments, left over after chemical cleaning and subsequent separation from the bacterial support, were observed to have accumulated preferentially at defect sites. This phenomenon facilitated an increase in selectivity toward alkenic products of up to 1.4 during hydrogenation of the alkyne. When biogenic NPs of platinum supported upon bacterial biomass were also investigated, they too were found to be active and selective although selectivity toward 1,4-butanediol was optimized only after the particles were chemically cleaned and separated from the biomass. Bi-poisoned 5% Pt on graphite, although highly selective, gave half the reaction rate of the biogenic counterpart (20% and 45% conversion of starting material respectively after 2 h), but the latter exhibited less selectivity for butanediol (0.7 and 0.9 respectively). It is proposed therefore that such biogenic materials may potentially act in a similar manner to Lindlar-type catalysts, used extensively in organic synthesis for selective hydrogenation of alkynes, in which an additive partially poisons metal sites but without the associated hazards of toxic heavy metals such as lead being present.

KEYWORDS: platinum bionanoparticles, bismuth, selective hydrogenation, alkynes, voltammetry



1. INTRODUCTION

Platinum has long been known to be a highly active catalyst for a number of important chemical transformations,^{1–8} and much research has been conducted with the aim of improving its selectivity. Conventional catalysts use a wide variety of ligands to impart the metal with selectivity for a given reaction. An enormous number of ligand classes exist, ranging from the very simple (e.g., Me, CN, CO, Cl, Br) to the highly complex, multidentate architectures,^{9–12} and ligand development is still an area of much activity. However, recent work has shown that selectivity can be achieved for heterogeneous catalysts through control of metal particle size and topography, rather than via the use of ligand coordination. In partial alkyne hydrogenation it is known that alkyne hydrogenation is favored on terraces, while alkene hydrogenation or isomerization is favored on surface defect sites, such as corners or edges.^{13,14} Zaera showed that Pt{111} terraces favored double bond isomerization of *trans*- to *cis*-2-butene and that the reverse selectivity is observed on more open faces.¹⁵ This is of potential importance in the partial hydrogenation of edible oils as the *trans*-isomers of fatty acids are known to adversely affect multiple cardiovascular risk factors and contribute to an increased risk of coronary heart disease.¹⁶

Differences in the catalytic activity of equally sized nanoparticles (NPs) of platinum with different shapes were reported by Schmidt et al.¹⁷ Three types of NPs, dominantly cubic, cubooctahedral, and octahedral, were shown to be equally active and selective for racemic hydrogenation of ethyl pyruvate in the absence of chiral modifier. However, when cinchonidine or quinine were added as chiral modifier, the reaction was both faster and more selective with increasing ratio of Pt{111}/Pt{100} terrace sites. The observed structure sensitivity was explained by a stronger adsorption of the cinchonidine upon a Pt{100} than a {111} face and a faster rate of hydrogenation of the modifier over the former surface, which leads to modifier degradation and a reduction in the number of chiral sites on the metal. Thus, for a given particle size range, a catalyst consisting of Pt{111} terraces is preferred for the enantioselective hydrogenation of ethyl pyruvate.

Jenkins et al.¹⁸ also showed that a platinum surface could give rise to changes in rate and enantiomeric excess for ethyl pyruvate hydrogenation by selectively poisoning step or terrace sites with bismuth or sulfur adatoms. The bismuth preferen-

Received: November 3, 2011

Revised: January 29, 2012

Published: February 17, 2012

tially adsorbed on step and {100} terrace sites, and catalysts selectively poisoned in this way were seen to have substantially increased activity in ethyl pyruvate hydrogenation, at the expense of reduced enantiomeric excess (ee)¹⁸ in contradiction of the conclusion of Schmidt et al.¹⁷ Pt/graphite catalysts poisoned with sulfur, selectively at {111} terraces, showed the opposite trend with improved ee but reduced activity.

More work on selective catalyst poisoning was reported by Anderson's group,¹⁴ who studied the effects of various poisons for palladium catalysts in alkyne hydrogenation to elucidate the roles of various surface sites on the reaction. Through selective poisoning of Pd edge sites with Bi, the group was able to show that the C–C triple bonds of the terminal alkyne 1-hexyne were hydrogenated upon terraces, while the resulting terminal alkene products were further hydrogenated on edges. Thus, in the hydrogenation of 1-hexyne, selectivity toward 1-hexene could be greatly improved by adding bismuth to a palladium catalyst. Also, experiments using an internal alkyne, 2-hexyne, supported Zaera's observation on platinum¹⁵ that cis-trans double bond isomerization of 2-hexene was favored over Pd terraces, rather than edges and defects. Selective poisoning of the Pd catalyst with Pb gave the reverse effect of Bi, blocking terraces and therefore resulted in improved selectivity toward the major product of 2-hexyne hydrogenation, *cis*-2-hexene.

As more is learned about structure sensitivity in catalytic reactions it becomes more evident that not only is metal selection important but also the size and topography of the metal particles can be crucial to achieving optimal activity and selectivity. Use of selective poisons is an effective way of tuning a given catalyst, but the utilization of toxic metals, such as lead, on a large scale or in the production of pharmaceuticals is clearly undesirable. Nonetheless, so-called "Lindlar" catalysts, based on selective poisoning of palladium metal catalysts by lead are employed extensively in organic synthesis to facilitate the hydrogenation of alkynes to alkenes with high selectivity.^{13,19,20} Selective hydrogenation is a significant area of research. Several recent papers and reviews have reported the main catalytic features of this structure sensitive surface reaction.^{21–35} In particular, particle size effects and structure sensitivity,^{21–28} the role of surface and subsurface hydrogen,³⁰ carbide phases,²⁹ ensemble size of the adsorption site,^{31–33} oligomerization side reactions,³⁴ the role of modifiers in promoting selectivity,^{14,35} and the position of the alkyne substituent on the substrate impact the overall reactivity and/or selectivity.³⁵

The preparation of nanoparticulate precious metals supported upon bacterial biomass has been previously reported in the literature.^{36,37} A culture of bacteria can be used to extract metal from a salt solution and deposit it as NPs on their surface, reducing the metal ion in the process. A number of metals, including Pd, Pt, Au, and Fe, can be successfully processed in this way, and a wide variety of bacteria may be used. The metal may be recovered from secondary sources, such as electronic scrap or waste catalysts and jewelry. NPs of palladium, or "bio-Pd", have been shown to be active in chromate reduction, Heck coupling, and both pentyne and butynediol hydrogenation.^{38,39}

Here we report two routes to improved selectivity in 1,4-butynediol hydrogenation using Pt catalysts: selective poisoning of platinum step sites with bismuth or with residual bacterial biomass. In the latter case, platinum NPs are first deposited on the surface of bacterial cells, which are then dried and ground into a powder before chemical processing removes the majority of the biomass, especially from terrace sites. The aim of the

work is to test the hypothesis that Pt heterogeneous catalysts sourced from bacteria may afford selectivities competitive with existing inorganic analogues based on Pb or Bi modified catalysts. Selective poisoning of a catalyst achieved using residual biomass, rather than elements such as Pb or Bi, would be advantageous because of its reduced toxicity. Pt has been used instead of Pd in this context because of the more straightforward manner in which electrochemical adsorption features may be interpreted and therefore it is emphasized that the present catalysts are meant to be seen as model systems and not directly reflecting the selectivity of "real" Pd-based Lindlar catalysts. In addition, complexities associated with subsurface hydrogen are avoided using Pt instead of Pd.

2. EXPERIMENTAL SECTION

2.1. Preparation of Platinum NPs Supported on Bacterial Biomass. Cells of *Escherichia coli* were grown and harvested as described previously.⁴⁰ A known volume of the concentrated resting cell suspension was transferred under OFN (oxygen free nitrogen) into 200 mL serum bottles, and an appropriate volume of a pre-prepared degassed 2 mM Na₂PtCl₆ solution was added in HNO₃, pH 2.0 so that the final ratio (weight of Pt/dry weight of cells) was 1:4 to give a final loading of 20% Pt on biomass. Cells/Pt mixtures were left to stand for 30 min at 30 °C with occasional shaking to promote biosorption of Pt(IV) complexes⁴⁰ before H₂ was sparged through the suspension for 10 min (0.2 atm) to reduce cell surface-bound Pt(IV) into Pt (0). The Pt(0)-coated biomass (bio-Pt) was harvested by centrifugation (3000 g, 10 min, 25 °C) and washed three times in distilled water (dH₂O). Following a final acetone wash, the black precipitate was resuspended in 5 mL of acetone and left to dry in air overnight. The resulting black powder containing bio-Pt(0) was finely ground in a mortar and tested for catalytic activity without any further processing.

2.2. Electrochemical Apparatus. A three-electrode electrochemical cell, described in detail previously⁴¹ was used, and data was recorded versus a Pd/H reference electrode and a platinum counter electrode. Voltammetric data was recorded in degassed 0.5 M aqueous sulphuric acid (Aristar) at a sweep rate of 50 mV/s unless otherwise stated. The glassy carbon (GC) support electrode used for analyzing the bio-Pt samples was cleaned and polished using alumina prior to use, and a cyclic voltammogram (CV) of the clean glassy carbon support electrode was recorded to verify cleanliness.

2.3. Chemical Treatment of 1% and 20% Bio-Pt NPs (*E. coli*) and Separation from Biomass. NPs were precleaned by placing into an aqueous solution of NaOH (~6M) for 6–8 weeks followed by multiple water rinsing/separation steps.⁴² Separation involved centrifugation to separate solid NPs from the aqueous liquid phase layer and subsequent removal of the aqueous phase using a pipet. Ultrapure water (18.2 MΩ cm) was then added, and the process repeated until all biomass was removed and the pH remained constant at 7. After precleaning, the NPs were rinsed once again with ultrapure water, and ~10 μL of the resulting suspension was deposited onto the polished and cleaned glassy carbon electrode. The droplet of NPs on the supporting electrode was then allowed to dry in air, and the CV profile of the NPs was recorded.

2.4. Preparation of Pt/C Catalyst Selectively Poisoned with Bismuth. Between 0.3 and 0.5 g of 5% platinum/graphite (Johnson Matthey) was stirred with an aqueous 10⁻³ M

Bi(NO₃)₃ solution for 3 h, filtered, rinsed thoroughly, and then air-dried.¹⁸ Different volumes of the Bi solution were added to generate varying levels of bismuth coverage. Some catalysts were then further dried in a furnace at 500 K for 3 h under 5% H₂/Ar(g). The Bi coverage was determined by cyclic voltammetry.⁴³ CVs of the catalysts were obtained by pressing a small amount of sample (5 mg) onto a platinum mesh (flamed-annealed and cleaned prior to use) which then formed the working electrode. Test CV data was collected in the same electrolyte as for the biogenic Pt NPs supported on the GC electrode.

2.5. Hydrogenation of 2-Butyne-1,4-diol. To a 500 mL Buchi reactor were added 2-propanol (300 mL), 2-butyne-1,4-diol (4 g), and platinum catalyst (0.400 g 5 wt % Pt/C or 0.100 g 20 wt % bio-Pt), and the mixture was purged with nitrogen gas. The mixture was then heated to 40 °C at a stirring speed of 1000 rpm (Rushton turbine) before pressuring the reactor with 2 bar of hydrogen. The mixture was stirred at 40 °C for the required reaction time. Samples were taken periodically throughout the reaction via a sampling valve for analysis by gas chromatography. All of the hydrogenation reactions are normalized to the same mass of platinum.

2.6. Gas Chromatography. Sample analysis was performed by gas chromatography, using a Varian CP-3380 with a flame ionization detector and a 25 M Chrompack Plot CP7576 capillary column with an Al₂O₃/KCl coating. The oven temperature ramp used was as follows: initial temperature of 95 °C for 30 min, ramp to 220 °C at 50 °C min⁻¹, hold 20 min. An injection volume of 0.1 μL was used.

3. RESULTS AND DISCUSSION

3.1. CV Characterization of Catalysts. To verify the surface state of the Bi/Pt and biogenic Pt prior to testing in the hydrogenation apparatus, CV data was recorded after two to three potential cycles from 0 to 0.85 V (Pd/H). In Figure 1 is shown the data collected for increasing coverage of bismuth deposited on the 5% Pt on graphite catalyst. The CV profile of the unmodified 5% Pt/graphite catalyst is very similar to that reported previously.^{18,43,44} In addition, previous character-

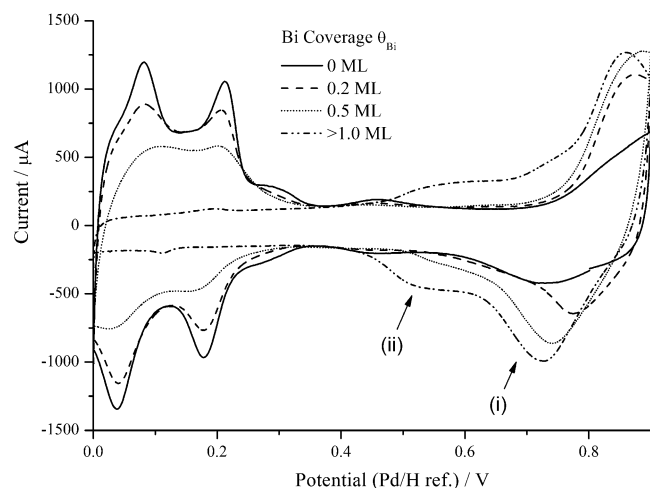


Figure 1. CV profiles of 5% Pt/graphite with increasing bismuth loadings (air-dried), recorded in 0.5 M sulphuric acid, sweep rate 50 mV/s. Peak (ii) corresponds to bismuth surface redox sites on {111} terraces whereas peak (i) corresponds to all other bismuth adsorption sites.

ization of the catalyst particle morphology as a function of temperature using TEM¹⁸ has demonstrated that it consists of clusters of connected Pt particles of average size 14 nm in diameter. CO chemisorption⁴⁴ has revealed a typical Pt surface area of 2.1 m²/g and from Brunauer–Emmett–Teller (BET) surface area measurements, a graphite support area of 10 m²/g was determined. The systematic blocking of Pt adsorption sites by bismuth is revealed by a decrease in peak area between 0 and 0.5 V as bismuth coverage is increased. The coverage of bismuth is expressed as the fraction of hydrogen underpotential deposition (H UPD) sites blocked, that is, complete attenuation of clean surface electroadsorption peaks between 0 and 0.4 V would correspond to 1 monolayer.⁴¹ As reported previously, preferential deposition of bismuth at steps sites (diminution of peaks at 0.05 V and 0.20 V) is observed and finally adsorption at Pt{111} terrace sites (quenching of broad CV feature at 0.5 V). However, because of the magnitude, shape, and potential of the 0.5 V peak, it may be deduced that the average terrace width is small (<3–4 Pt atoms⁴⁵) and that the majority of surface sites are steps or defects. This is in accordance with the small magnitude of the broad peak at 0.6 V which forms at highest bismuth loadings that may be ascribed exclusively to a redox process of bismuth adsorbed on {111} terraces.^{46,47} This peak is only observed at high bismuth coverages after nearly all clean surface step sites are blocked. The bismuth redox peak at defect sites is observed at potentials >0.8 V and is seen to increase in magnitude as bismuth coverage increases.⁴⁷ For the 5% Pt/graphite catalyst sintered under hydrogen at 500 K (Figure 2), a marked change in the

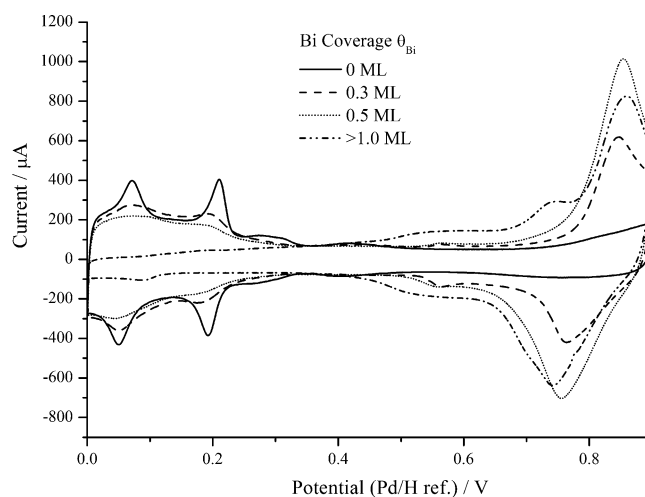


Figure 2. CV profiles of 5% Pt/graphite with increasing bismuth loadings (sintered at 500 K in 5% H₂, Ar(g)), recorded in 0.5 M sulphuric acid, sweep rate 50 mV/s.

clean surface CV is observed in relation to the unsintered sample depicted in Figure 1. In particular, both {100} (shoulder at 0.2–0.33 V) and {111} terrace sites (peak at 0.4 V) are more marked and peak shapes indicate larger terraces have developed (in the case of Pt{111}, the broad peak at 0.5 V corresponding to bisulphate adsorption has shifted to more negative potentials⁴⁵). Coupled with these changes is a decrease in the peak width of the defect sites at 0.08 and 0.2 V. This phenomenon has been reported previously and corresponds to a change from clusters of randomly shaped and connected Pt NPs to larger, faceted, and hexagonal Pt NPs.⁴³ In spite of these morphological differences, the uptake of bismuth onto the Pt

nonetheless follows the same sequence as for the unsintered catalyst in that step site peaks are first blocked followed by the development of a peak (now sharper and more intense than before) ascribable to bismuth adatoms adsorbed on Pt{111} terraces (0.55 V). In Figure 3 is shown the CV of the Pt NPs

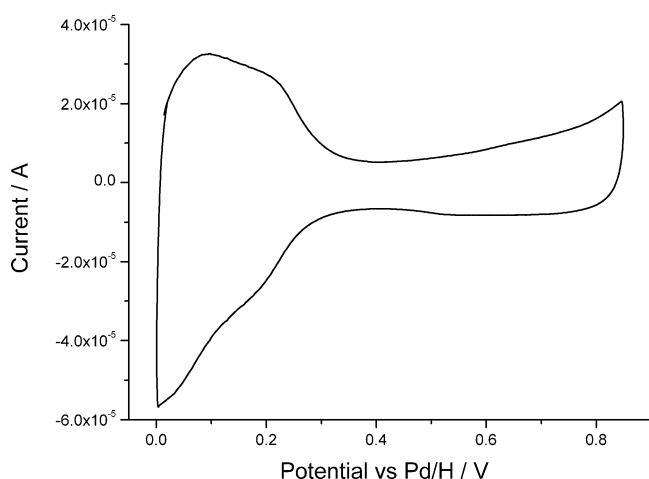
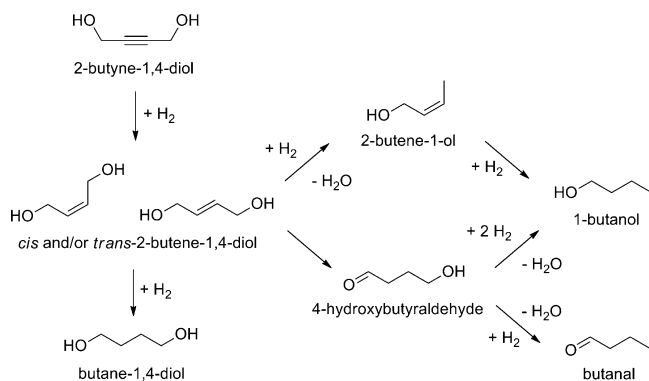


Figure 3. CV recorded for precleaned 20% bio-Pt (derived from *E. coli*) supported on a glassy carbon electrode, in 0.1 M sulphuric acid, sweep rate 50 mV/s.

that have been liberated from the *E. coli*. It is seen that in this case the defect sites at 0.05 and 0.22 V are strongly attenuated (although some intensity is still present). The 20% Pt bioNPs have been examined previously and cleaned electrochemically to various degrees of surface cleanliness after separation from the bacterial host.⁴² The 20% Pt bioNPs were found to exhibit rather narrow {111} terraces as signified by a weak and broad Pt{111} electroadsorption feature at 0.5 V when completely clean. This feature may also be discerned in Figure 3 on the negative going potential sweep of the initial CV cycle. However, it is obscured on the positive sweep by a weak electroadsorption feature at 0.65 V indicating that some adsorbed organic material may still undergo electrooxidation.

3.2. Selective Hydrogenation of 1,4-Butynediol. The hydrogenation of 1,4-butyne diol was used as a model reaction to assess the catalytic activity of NPs of platinum supported on carbon or the surface of bacterial biomass (bio-Pt). The possible products of the reaction are shown in Scheme 1. The four products formed from butynediol besides 1,4-butanediol,

Scheme 1. Reaction Pathway for 2-Butyne-1,4-diol Hydrogenation



specifically 2-buten-1-ol, 4-hydroxybutyraldehyde, 1-butanol, and butanal, are hereafter collectively referred to as side-products in this paper.

3.2.1. Sintered vs Nonsintered Pt/C. One common method of altering metal particle size and shape is sintering. Heating a heterogeneous precious metal catalyst leads to changes in metal distribution and morphology, leading to an increased average metal particle size.^{48,49} There are two generally accepted mechanisms for particle growth: Ostwald ripening⁵⁰ and particle migration and coalescence,⁵¹ often both occur during sintering. As the temperature is increased the particles may migrate a greater distance over the surface of the support.⁵² The presence of reducing or oxidizing conditions, because of an atmosphere of H₂ or O₂ for example, can also affect the degree of migration.^{52,53} Changes in the morphology of the metal particles accompany the changes in size, and increasing temperatures may lead to formation of increasingly crystalline particles.^{43,54} The nature of the support material may also affect particle migration, as a higher support-metal interaction reduces migration and limits particle size.⁵⁵ Changes in the proportion of terraces, kinks, corners, and adatoms can also lead to changes in catalyst activity or selectivity.¹⁸

To elucidate structure–reactivity relationships in 1,4-butyne diol hydrogenation, the sintered and unsintered heterogeneous platinum catalysts were tested for the reaction.

The resulting reaction profiles are shown in Figure 4. Under the conditions used, the unmodified Pt/C catalyst shows complete alkyne conversion in just over 1 h (Figure 4A). The *cis*-form of 1,4-butyne diol is initially the major product of the reaction, until the concentration of starting material is low and the butenediols are further reacted to form butanediol or the various side-products.

When the catalyst is sintered at 500 K (Figure 4B), the initial rate is increased but complete conversion of the alkyne occurs at around the same time as for the nonsintered catalyst. There is also a change in the product distribution at alkyne conversions above 40%. While alkyne is still present in the mixture, the *cis*-butenediols selectivity is higher than that observed with the nonsintered catalyst, but the *cis*-/*trans*-ratio is lower suggesting a greater degree of isomerization. Butenediols selectivity is higher after sintering at 500 K (Figure 5); the amount of butanediol is increased, and the amount of other side products is reduced. This suggests that the further hydrogenation and the formation of the other side products occur on different active sites on the surface of the catalyst and that sintering results in a change in the proportion or availability of the sites responsible for further hydrogenation of the alkyne. These results agree with an increase in the proportion of terrace sites to steps/kinks after sintering, as confirmed by CV, and also suggest that the reaction pathways leading to formation of side-products (those other than butanediol) occur on defect sites.^{13,14}

3.2.2. Pt/C Selectively Poisoned with Bi. A series of Pt/graphite catalysts with increasing amounts of Bi were tested to determine the effect of poisoning on rate and selectivity. The results for the unmodified Pt/graphite catalyst are described above (Figure 4 and 5). When Pt catalyst is poisoned with a small amount of bismuth (0.2 monolayers, Figure 6A), the selectivity toward butenediols with respect to 1,4-butanediol and side-products is increased by around 10% for alkyne conversions above 20%. Formation of side products and 1,4-butanediol is suppressed until the majority of the alkyne is consumed. However, the rate of alkyne hydrogenation is also

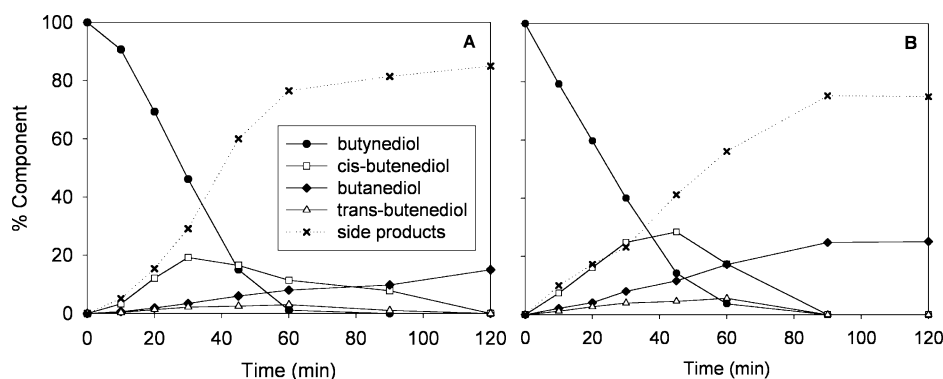


Figure 4. Kinetic data for 1,4-butyne diol hydrogenation obtained using an unsintered 5%Pt/graphite catalyst (A) and catalysts sintered at 500 K (B) in argon/hydrogen atmosphere. Data shown are from a representative experiment; errors between experiments are not shown but were within 5%.

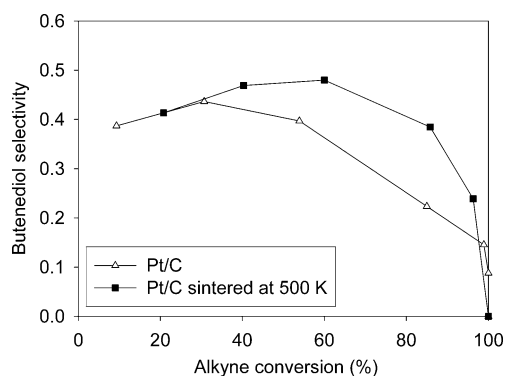


Figure 5. Butynediol selectivity using sintered and nonsintered 5% Pt/graphite catalyst.

reduced, with total 1,4-butyne diol conversion being reached at around 100 min rather than 60 min. Further increasing the degree of bismuth-poisoning on the catalyst resulted in improved selectivity at the expense of activity. The more Bi-poisoned catalyst (0.5 monolayers) gave a very low rate of reaction but 100% butynediol selectivity (Figure 6B) and the catalyst with the greatest amount of bismuth (>1 monolayer) was totally inactive in the reaction (not shown). The large increase in selectivity coincides with bismuth blocking of all step peaks in the CV of the catalyst. Hence, the observed trend is attributed to reduction in the surface density of free step sites on the catalysts by selective poisoning with bismuth. These step sites are reported to be the locations responsible for hydrogenation of carbon-carbon double bonds,¹³ while triple

bond hydrogenation occurs on terraces. Thus, selectively blocking steps on the Pt surface limits further reaction of butynediol but, as the terraces are left open, butynediol hydrogenation may still occur. As the amount of bismuth added to the platinum catalyst is increased there is a greater propensity for blocking of terrace sites and alkyne conversion will therefore be reduced. Figure 7 summarizes changes in selectivity as a function of bismuth coverage.

Figure 7B depicts the trends in selectivity to 1,4-butyne diol versus conversion as a function of bismuth loading for the 5% Pt/graphite catalyst sintered in hydrogen at 500 K. As seen in the unsintered case, a general increase in selectivity is observed as more bismuth is added to the surface although at the cost of a decrease in overall activity. Again, the complete blockage of defect sites by bismuth leads to the greatest selectivity although in this instance, the fully blocked catalyst exhibiting the lowest activity gave rise to the highest selectivity (close to 100%).

The ratio of *cis*- to *trans*-1,4-butyne diols is largely unaffected by the degree of bismuth poisoning or sintering and selectivity toward the *cis*- product is around 90% for both series of catalysts (not shown), attributable to the fact that *cis*- to *trans*-isomerization occurs on extensive terraces¹⁴ and hence is not inhibited by selective poisoning of Pt steps.

3.2.3. Biogenic bio-Pt and Electrochemically Cleaned bio-Pt. Two types of biogenic platinum catalysts were also tested in the hydrogenation. The first consists of NPs of platinum supported on bacterial biomass that is dried and ground to a powder (bio-Pt). The second is produced through chemical processing of the former, which removes the majority of the biomass from the metal particles. Figure 8 shows hydrogenation

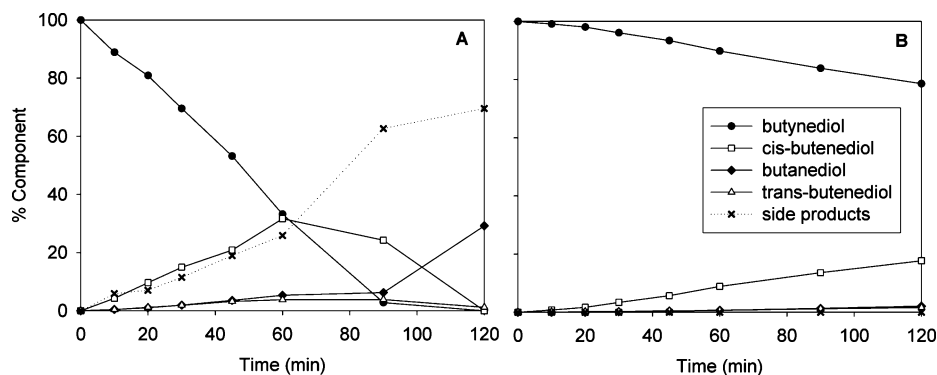


Figure 6. Kinetic data for 1,4-butyne diol hydrogenation obtained for unsintered 5%Pt on graphite catalyst modified with 0.2 monolayers (A) or 0.5 monolayers (B) of bismuth (see text for definition of monolayer).

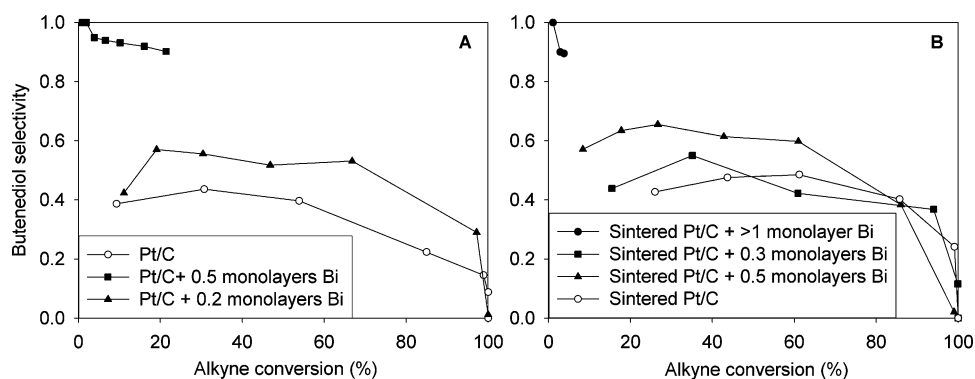


Figure 7. Butenediol selectivity using unsintered (A) and sintered (B) 5%Pt/graphite catalysts with varying amounts of adsorbed Bi.

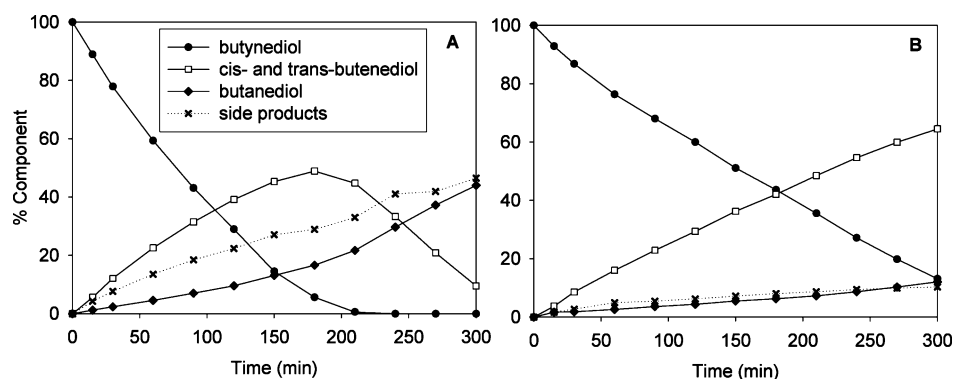


Figure 8. Kinetic data for 1,4-butyne diol hydrogenation using bio-Pt NPs supported on (A) native *E. coli* cells and (B) chemically treated and separated from the bacterial host. Surface structure and composition of bio-NPs corresponds to that depicted in CV in Figure 3.

data for both the bio-Pt and chemically processed bio-Pt with the biomass component removed respectively. When compared with data for the unsintered Pt/graphite and the best Bismuth modified unsintered Pt/graphite catalyst (Figure 9) it is evident

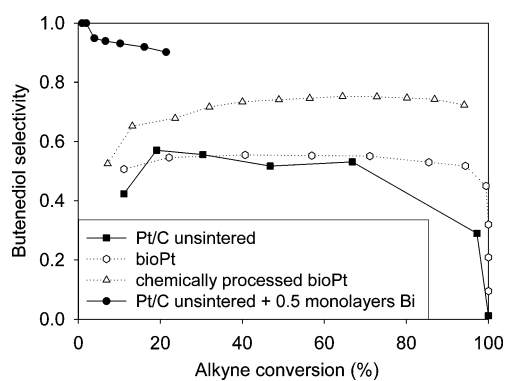


Figure 9. Butenediol selectivity versus alkyne conversion using four different platinum catalysts with increasing occupation/blockage of defect sites.

that a general trend of increasing selectivity is obtained as more and more Pt defect sites are blocked. The slightly higher selectivity toward alkenic products exhibited by the bio-Pt compared to unsintered catalyst may be due to either the influence of the catalyst support or the overall surface morphology of the Pt NPs. Nonetheless, it is surprising that a Pt surface embedded within a bacterial particle is almost as unselective as an unsintered Pt/graphite catalyst up to 70% conversion, whereas at between 70 and 90% conversion

selectivity is maintained with the bio-Pt but is reduced with the inorganic counterpart. It suggests that *practically all adsorption sites are available to Pt supported on bacteria, that is, selective blocking of defect sites is minimal*. In the situation involving the same NPs free of the bacterial particles but selectively blocked with organic residues, a marked increase in selectivity is observed (Figure 9) but at the expense of reaction rate; whereas the reaction rate of the “cleaned” bio-Pt (Figure 8B) is double that of the chemical counterpart modified with 0.5 monolayers of bismuth (Figure 6B). In the limit of complete blocking of defect sites by bismuth, the highest selectivity is obtained.

3.3. Discussion. A series of Pt catalysts derived from biological and inorganic sources have been investigated in relation to their selectivity toward the hydrogenation of 1,4-butyne diol. The general finding is that blocking of defect sites in preference to terraces affords an increase in the selectivity toward alkenic products. This general finding is in accordance with both previous studies^{13,14} and in particular confirms that defect sites appear to be highly active in the hydrogenation of alkenic intermediates. It should be noted, however, that at the highest conversions of reactant (>60%), selectivity tended to decrease. This was particularly true of both the unsintered and the sintered Pt/graphite catalysts (Figures 7 and 9). Here, it is assumed that in excess of starting material, defect sites are preferentially blocked by the reactant itself such that subsequent hydrogenation of the alkenic intermediate product is prohibited by competitive adsorption of the alkyne substrate. In the case of the bismuth-poisoned sintered and unsintered catalysts, this phenomenon also appears to be taking place in spite of the fact that the defect sites tend to be blocked already

by bismuth. Two reasons for this observation may therefore be hypothesized. The first is that the alkenic product may displace some bismuth at steps under hydrogenation conditions whereas at low conversions, this process is limited. If correct, this predicts a loss of bismuth to the liquid phase as reaction proceeds and a subsequent decrease in selectivity as step sites become available. In the second hypothesis, alkene hydrogenation may take place even on {111} terraces but only in the absence of the starting alkyne (which otherwise competes more successfully than alkene for these terrace sites). Again, as more and more alkyne is consumed, it becomes possible for alkene to be converted to the alkane at terraces even though defect sites are unavailable since they are blocked by bismuth.

This study has shown that 20% Pt on bacterial biomass has a comparable selectivity to that of 5% Pt on carbon up to 70% conversion, with, in contrast to the nonbiological counterpart, selectivity being retained at up to reaction completion. This suggests a fundamental difference between the Pt catalysts of chemical and biogenic origin (although 20% Pt on graphite was not tested). However, in what is believed to be a new finding, the role of the bismuth adatom in facilitating selectivity may be mimicked by a nonmetallic fragment so long as it is retained at defect sites after “cleaning”, with the reaction rate being twice that of the bismuth-treated chemical counterpart. The nature of this organic fragment, derived from the bacterial particle used to nucleate the bio-Pt NPs, remains unknown although it is extremely resilient toward both reduction and oxidation (according to CV) and may only be removed at potentials in excess of 1 V (Pd/H).⁴² This behavior is similar to that reported by Garcia et al. for palladium catalysts modified with amines and nitriles³⁵ although the adsorption site was not determined explicitly in this case. Hence, judicious control of the level of residual contamination of chemically processed bio-Pt may afford a new and direct route to highly selective hydrogenation catalysts that avoids the use of any toxic heavy metal components.

It should also be noted that the present studies used bio-Pt NPs manufactured on and purified from native cells of *E. coli*. Previous work using mutants deficient in key enzymes involved in metallic NP synthesis has “redirected” bio-Pd NPs to, accordingly, different cellular locations in cells of *Desulfovibrio fructosovorans*⁵⁶ and *E. coli*,⁵⁷ with the resulting catalytic activity (determined by reduction of Cr(VI) to Cr(III)) increased⁵⁸ or decreased,⁵⁷ respectively. The current study shows the high importance of the biochemical fragment in the catalytic property of the final nanomaterial and future studies would aim to identify the nature of the biomass fragment as the starting point for “designer” catalyst manufacture by a combination of molecular genetics and post-manufacturing approaches.

4. CONCLUSIONS

Our results show that selective poisoning using varying amounts of bismuth can allow tuning of the selectivity of a heterogeneous catalyst without the use of complex ligands or formation of tailor-made particle morphologies. Bismuth preferentially adsorbs upon defect sites of the metal surface, thus inhibiting reactions which are favored on these sites. Once the amount of poison is in excess of the number of defect sites, the bismuth will cover the terraces of the metallic NP, and catalytic activity will eventually be suppressed. The poisoning experiments suggest that hydrogenation of the carbon–carbon

triple bond occurs largely on terraces while the alkene reacts mainly on steps or kinks but isomerizes over terraces.

A biogenic catalyst, consisting of Pt NPs supported upon bacterial biomass, gave slightly superior selectivity than an unsintered Pt/C catalyst, possibly attributable to partial blocking of defect sites by the bacterial matrix. However, the conclusion from the small degree of difference in selectivity for both catalysts suggests that most sites for hydrogenation in the bacterial supported Pt are still available. When the majority of biomass is chemically removed, the selectivity of the resulting Pt particles is greatly improved, in a similar manner to that observed with selective poisoning from Bi. The results suggest that the biomass is selectively removed from terraces thus enhancing the rate of reactions occurring on those sites, that is, alkyne to alkene hydrogenation.

The reaction selectivity, coupled with retention of an acceptable reaction rate, enables the conclusion that biogenic Pt-NPs act as selective catalysts for alkyne hydrogenation but, unlike for Lindlar-type catalysts, without the addition of toxic metals to achieve this outcome.

AUTHOR INFORMATION

Corresponding Author

*E-mail: j.wood@bham.ac.uk. Phone: +44 (0) 121 414 5295. Fax: +44 (0) 121 414 5324.

Notes

The authors declare no competing financial interest.

REFERENCES

- (1) Vedernikov, A. N. *Curr. Org. Chem.* **2007**, *11*, 1401–1416.
- (2) Liu, C.; Bender, C. F.; Han, X.; Widenhoefer, R. A. *Chem. Commun.* **2007**, *35*, 3607–3618.
- (3) Bartok, M. *Curr. Org. Chem.* **2006**, *10*, 1533–1567.
- (4) Lin, S. D.; Vannice, M. A. *J. Catal.* **1993**, *143*, 539–53.
- (5) Buergi, T.; Baiker, A. *Acc. Chem. Res.* **2004**, *37*, 909–917.
- (6) Korovchenko, P.; Donze, C.; Gallezot, P.; Besson, M. *Catal. Today* **2007**, *121*, 13–21.
- (7) Ikeda, S.; Ishino, S.; Harada, T.; Okamoto, N.; Sakata, T.; Mori, H.; Kuwabata, S.; Torimoto, T.; Matsumura, M. *Angew. Chem., Int. Ed.* **2006**, *45*, 7063–7066.
- (8) Antolini, E.; Lopes, T.; Gonzalez, E. R. *J. Alloys Compd.* **2008**, *461*, 253–262.
- (9) Moret, M.-E.; Chen, P. *Organometallics* **2008**, *27*, 4903–4916.
- (10) Mitton, S. J.; McDonald, R.; Turculet, L. *Organometallics* **2009**, *28*, 5122–5136.
- (11) Doherty, S.; Knight, J. G.; Smyth, C. H.; Harrington, R. W.; Clegg, W. *Organometallics* **2007**, *26*, 6453–6461.
- (12) Doherty, S.; Knight, J. G.; Smyth, C. H.; Harrington, R. W.; Clegg, W. *Organometallics* **2007**, *26*, 5961–5966.
- (13) Ulan, J. G.; Maier, W. F.; Smith, D. A. *J. Org. Chem.* **1987**, *52*, 3132–3142.
- (14) Anderson, J. A.; Mellor, J.; Wells, R. P. K. *J. Catal.* **2009**, *261*, 208–216.
- (15) Lee, I.; Morales, R.; Albitzer, M. A.; Zaera, F. *Proc. Nat. Acad. Sci. U.S.A.* **2008**, *105*, 15241–15246.
- (16) Mozaffaria, D.; Aro, A.; Willett, W. C. *Eur. J. Clin. Nutrition.* **2009**, *63*, S5–S21.
- (17) Schmidt, E.; Vargas, A.; Mallat, T.; Baiker, A. *J. Am. Chem. Soc.* **2009**, *131*, 12358–12367.
- (18) Jenkins, D. J.; Alabdulrahman, A. M. S.; Attard, G. A.; Griffin, K. G.; Johnstone, P.; Wells, P. B. *J. Catal.* **2005**, *234*, 230–239.
- (19) Gutmann, H.; Lindlar, H. *Chemistry of Acetylenes*; Marcel Dekker: New York, 1969.
- (20) Lindlar, H.; Dubuis, R. *Org. Synth. Coll.* **1973**, *5*, 880.
- (21) Studt, F.; Abild-Pedersen, F.; Bliigaard, T.; Sorensen, R. Z.; Christensen, C. H.; Norskov, J. K. *Science* **2008**, *320*, 1320–1322.

- (22) Garcia-Mota, M.; Gomez-Diaz, J.; Novell-Leruth, G.; Vargas-Fuentes, M. C.; Bellarosa, L.; Bridier, B.; Pérez-Ramírez, J.; López, N. *Theor. Chem. Acc.* **2011**, *128*, 663–673.
- (23) Lederhos, C. R.; Badano, J. M.; Quiroga, M. E.; L'Argentièrre, P. C.; Pascual, F. C. *Quím. Nova* **2010**, *33*, 816–820.
- (24) Lederhos, C. R.; L'Argentièrre, P. C.; Figoli, N. S. *Ind. Eng. Chem. Res.* **2005**, *44*, 1752–1756.
- (25) Bond, G. C.; Dowden, D. A.; Mackenzie, N. *Trans. Faraday Soc.* **1958**, *54*, 1537–1546.
- (26) Boitiaux, J. P.; Cosyns, J.; Robert, E. *Appl. Catal.* **1987**, *32*, 145–168.
- (27) Binder, A.; Seipenbusch, M.; Muhler, M.; Kasper, G. *J. Catal.* **2009**, *268*, 150–155.
- (28) Semagina, N.; Kiwi-Minsker, L. *Catal. Lett.* **2009**, *127*, 334–338.
- (29) Borodziński, A.; Bond, G. C. *Catal. Rev. Sci. Eng.* **2006**, *48*, 91–144.
- (30) Teschner, D.; Borsodi, J.; Wootsch, A.; Revay, Z.; Havecker, M.; Knop-Gericke, A.; Jackson, S. D.; Schlögl, R. *Science* **2008**, *320*, 86–89.
- (31) Molnar, A.; Sarkany, A.; Varga, M. *J. Mol. Catal. A: Chem.* **2001**, *173*, 185–221.
- (32) Krawczyk, M.; Sobczak, J.; Palczewska, W. *Catal. Lett.* **1993**, *17*, 21–28.
- (33) Guzzi, L.; Schay, Z.; Stefler, Gy.; Liotta, L. F.; Deganello, G.; Venezia, A. M. *J. Catal.* **1999**, *182*, 456–462.
- (34) Garcia-Mota, M.; Bridier, B.; Pérez-Ramírez, J.; López, N. *J. Catal.* **2010**, *273*, 92–102.
- (35) Garcia, P. E.; Lynch, A. S.; Monaghan, A.; Jackson, S. D. *Catal. Today* **2011**, *164*, 548–551.
- (36) Lloyd, J. R.; Yong, P.; Macaskie, L. E. *Appl. Environ. Microbiol.* **1998**, *64*, 4607–4609.
- (37) Creamer, N. J.; Mikheenko, I. P.; Yong, P.; Deplanche, K.; Sanyahumbi, D.; Wood, J.; Pollmann, K.; Merroun, M.; Selenska-Pobell, S.; Macaskie, L. E. *Catal. Today* **2007**, *128*, 80–87.
- (38) Bennett, J. A.; Creamer, N. J.; Deplanche, K.; Macaskie, L. E.; Shannon, I. J.; Wood, J. *Chem. Eng. Sci.* **2010**, *65*, 282–290.
- (39) Wood, J.; Bodenes, L.; Bennett, J. A.; Deplanche, K.; Macaskie, L. E. *Ind. Eng. Chem. Res.* **2010**, *49*, 908–988.
- (40) Yong, P.; Rowson, N. A.; Farr, P. G.; Harris, I. R.; Macaskie, L. E. *Biotechnol. Bioeng.* **2002**, *80*, 369–379.
- (41) Evans, R. W.; Attard, G. A. *J. Electroanal. Chem.* **1993**, *345*, 337–350.
- (42) Attard, G. A.; Casadesús, M.; Macaskie, L. E.; Deplanche, K. *Langmuir*, DOI: 10.1021/la204495z, accepted.
- (43) Attard, G.; Griffin, K. G.; Jenkins, D. J.; Johnston, P.; Wells, P. B. *Catal. Today* **2006**, *114*, 346–352.
- (44) Attard, G. A.; Gillies, J. E.; Harris, C. A.; Jenkins, D. J.; Johnston, P.; Price, M. A.; Watson, D. J.; Wells, P. B. *Appl. Catal., A* **2001**, *222*, 393–405.
- (45) Clavilier, J.; El-Achi, K.; Rodes, A. *Chem. Phys.* **1990**, *141*, 1–14.
- (46) Rodríguez, P.; Solla-Gullon, J.; Vidal-Iglesias, F. J.; Herrero, E.; Aldaz, A.; Feliu, J. M. *Anal. Chem.* **2005**, *77*, 5317–5323.
- (47) Clavilier, J.; Feliu, J.-M.; Fernandez-Vega, A.; Aldaz, A. *J. Electroanal. Chem.* **1989**, *269*, 175–189.
- (48) Susu, A. A.; Ogogo, E. O.; Ngomo, H. M. *Chem. Eng. Res. Des.* **2006**, *84*, 664–676.
- (49) Datye, A. K.; Xu, Q.; Kharas, K. C.; McCarty, J. M. *Catal. Today* **2006**, *111*, 59–67.
- (50) Fuentes, G. A.; Salinas-Rodríguez, E. *Stud. Surf. Sci. Catal.* **2001**, *139*, 503–510.
- (51) Pilyankevich, A. N.; Mel'nikova, V. A. *Poroshk. Metall.* **1982**, *9*, 68–74.
- (52) Sushumna, I.; Ruckenstein, E. *J. Catal.* **1988**, *109*, 433–462.
- (53) Chen, M.; Schmidt, L. D. *J. Catal.* **1978**, *55*, 348–360.
- (54) Harris, P. J. F. *J. Catal.* **1986**, *97*, 527–542.
- (55) Arai, M.; Ishikawa, T.; Nakayama, T.; Nishiyama, Y. *J. Colloid Interface Sci.* **1984**, *97*, 254–265.
- (56) Mikheenko, I. P.; Rousset, M.; Dementin, S.; Macaskie, L. E. *Appl. Environ. Microbiol.* **2008**, *19*, 61144–6146.
- (57) Deplanche, K.; Caldelari, I.; Sargent, F.; Macaskie, L. E. *Microbiology* **2010**, *156*, 2630–2640.
- (58) Rousset, M.; Casalot, L.; De Philip, P.; Belaich, A.; Mikheenko, I.; Macaskie, L. E. International Patent PCT/EP200/050942, 2006.